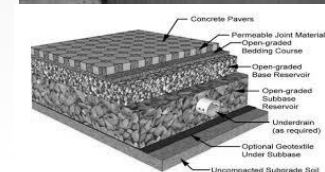
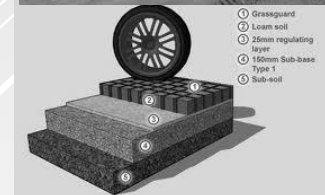
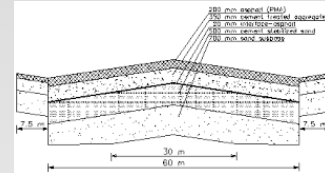


## LECTURE 8: Asphalt mixtures



## 8.1 Introduction

In order to be able to design the thickness of a flexible pavement, the stiffness and the fatigue resistance of the asphalt mixture used should be known. In this chapter we will discuss how information on these characteristics can be obtained.

## 8.2 Mixture stiffness

As explained previously, repeated load tests are needed to obtain the stiffness characteristics of asphalt mixtures in relation to the **loading time** and **temperature**. Tests which are suitable to determine the mixture stiffness are the 2 point, 3 point and 4 point bending test, the tension test, the tension – compression test and the indirect tension test. Figure 76 shows some of these tests.



4 point bending test



2 point bending test



direct tension test



indirect tension test

Figure 76: Examples of tests to determine mixture stiffness.

An example of the results of such tests is shown in figure 77.

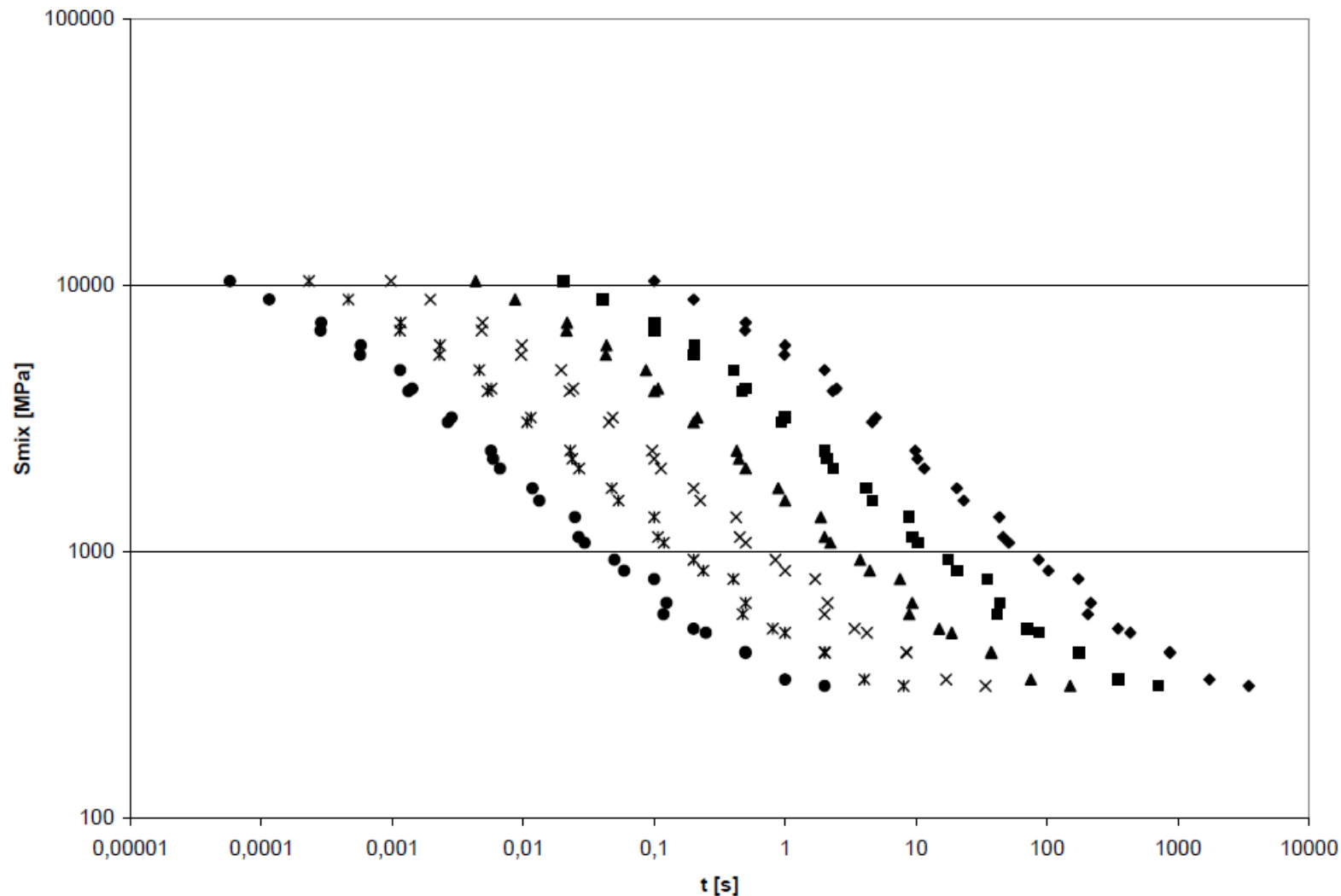


Figure 77: Example of the master curve for the mixture stiffness.

- the slope of the master curve is an important parameter since it reveals information on the fatigue and permanent deformation characteristics of the mixture.
- If testing of the mixture is too cumbersome, one can estimate the mixture stiffness by using one of the available nomographs to predict the mixture stiffness from the bitumen stiffness and the volumetric composition. Examples of such nomographs are those developed by Shell (figure 78 [31]) and the one developed by the Belgian Road Research Centre (figure 79 [32]). The bitumen stiffness can be obtained from e.g. dynamic shear rheometer tests (figure 80) that give the stiffness of the bitumen in relation to the loading time and temperature.



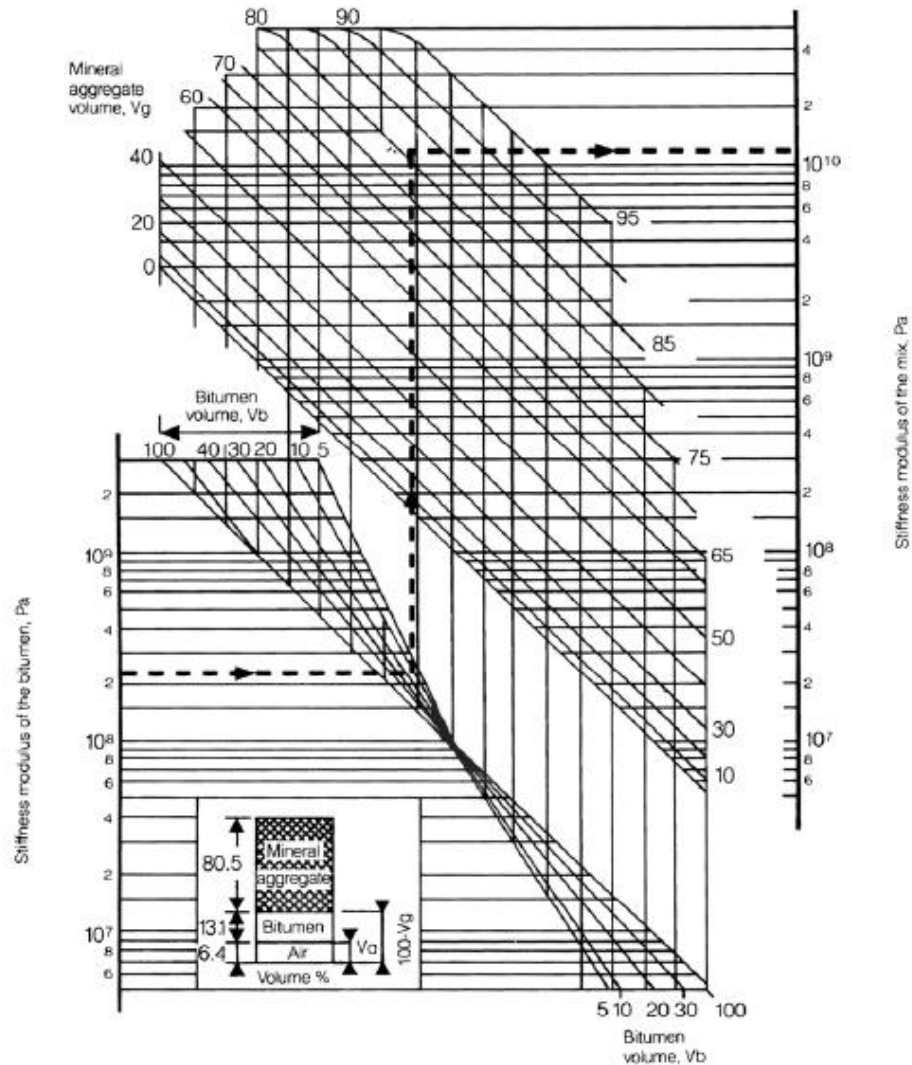


Figure 78: Shell nomograph to predict the stiffness of asphalt mixtures.

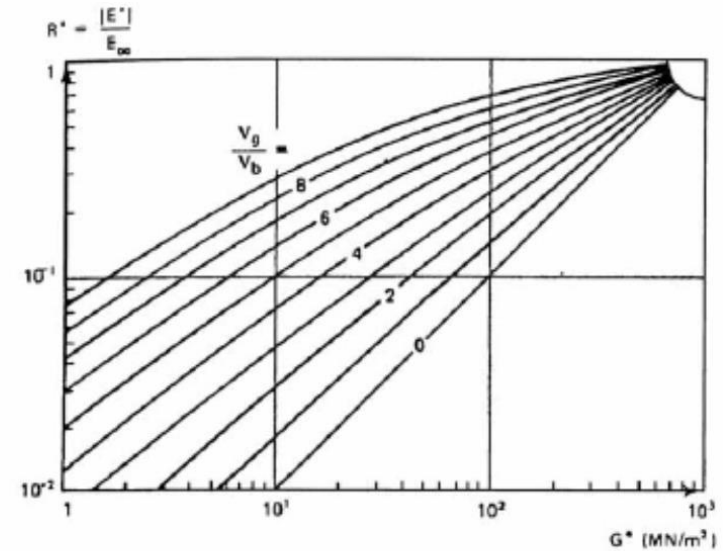


Figure 79: Nomograph of the Belgian Road Research Centre to predict asphalt mixture stiffness.

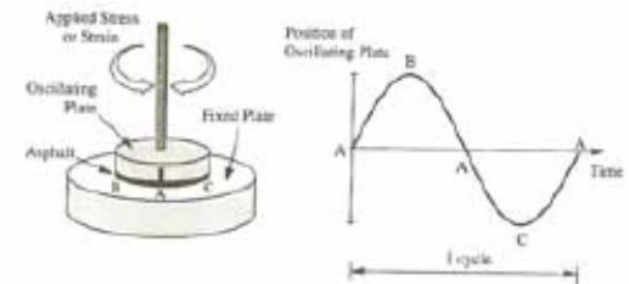


Figure 80: Principle of the dynamic shear rheometer test.

However, the bitumen stiffness can also be estimated from available nomographs. An example of such a nomograph is the one developed by Van der Poel of the Shell laboratories (figure 81 [31]). A much more attractive solution is to use the program BANDS produced by Shell to estimate the stiffness of the bitumen and the asphalt mixture as a function of the characteristics of the bitumen, the temperature and loading time as well as the volumetric composition of the mixture. When using the van der Poel nomograph one should realize that it has been developed some 30 years ago. Since that time bitumen production techniques have been changed implying that the nomograph might be a bit outdated. Indications for that are obtained by comparing experimentally determined data with those estimated through use of the nomograph. It seems that the experimentally determined values are somewhat higher and less dependent on the loading time than those predicted by means of the nomograph. One should also be aware of the differences that exist between the mixture stiffness estimation procedures. This will be illustrated by means of an example.

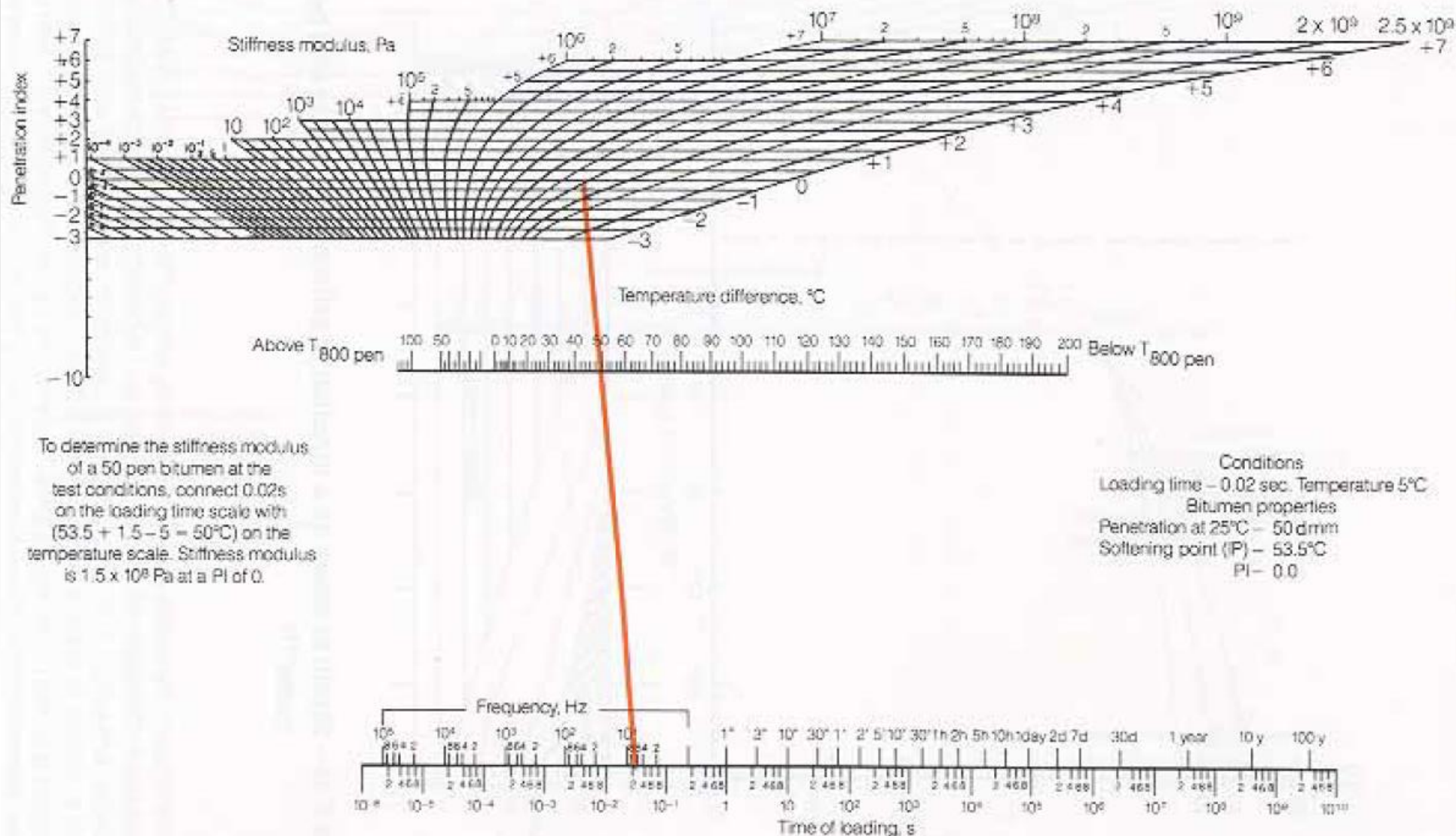


Figure 81: Van der Poel nomograph to predict the stiffness of the bitumen.

$$A = \frac{\log pen T1 - \log 800}{T1 - ASTM \text{ softening point}}$$

$$PI = \frac{20 (1 - 25A)}{1 + 50A}$$

PI is asphalt cement temperature susceptibility, range from -3 ( high temperature susceptible asphalt), +7 (low temperature susceptible asphalt)



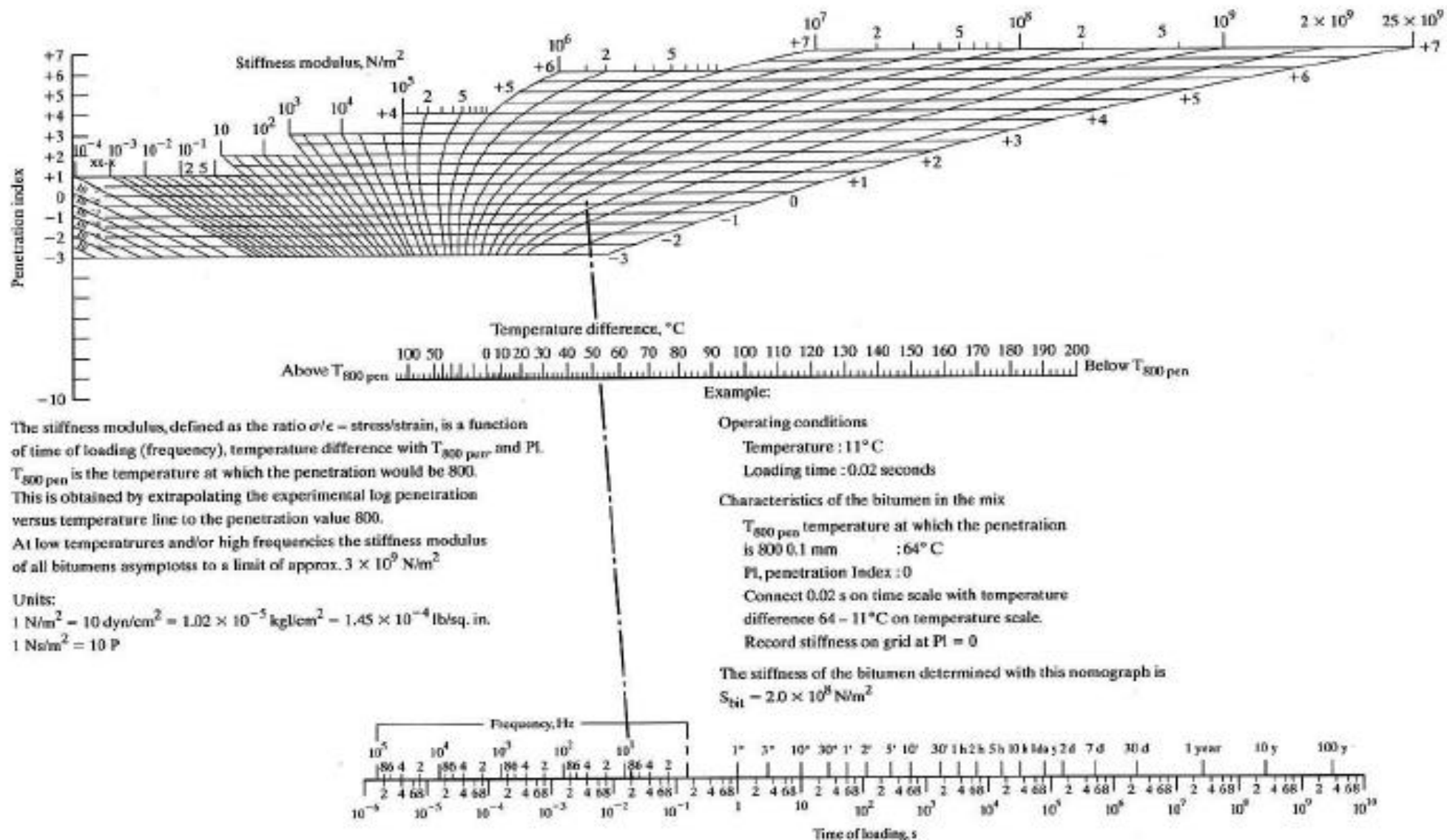


Figure 81: Van der Poel nomograph to predict the stiffness of the bitumen.

Let us assume we want to know the stiffness of an asphalt mixture with  $V_b = 10\%$ ,  $V_a = 5\%$  and  $V_g = 85\%$  (these are the volume percentage of bitumen, the void content and the volume content of mineral aggregates). According to the Belgium procedure we must first estimate the maximum stiffness of the asphalt mixture. This value is calculated using:

$$E_{\max} = 3.56 * 10^4 \{(V_b + V_a) / V_b\} e^{-0.1V_a} = 32414 \text{ MPa}$$

Then we use figure 79 assuming a shear modulus of 10 MPa. Since  $V_g / V_b = 8.5$  we obtain an asphalt stiffness of:

$$E^* = 0.25 * 32414 = 8103 \text{ MPa}$$

If we use figure 78 we need to know  $S_{\text{bit}}$ . For reasons of simplicity we assume that

$$S_{\text{bit}} = E^* = 3 * G^* = 30 \text{ MPa}.$$

Using figure 78 we obtain  $S_{\text{mix}} = E^* = 5000 \text{ MPa}$ .

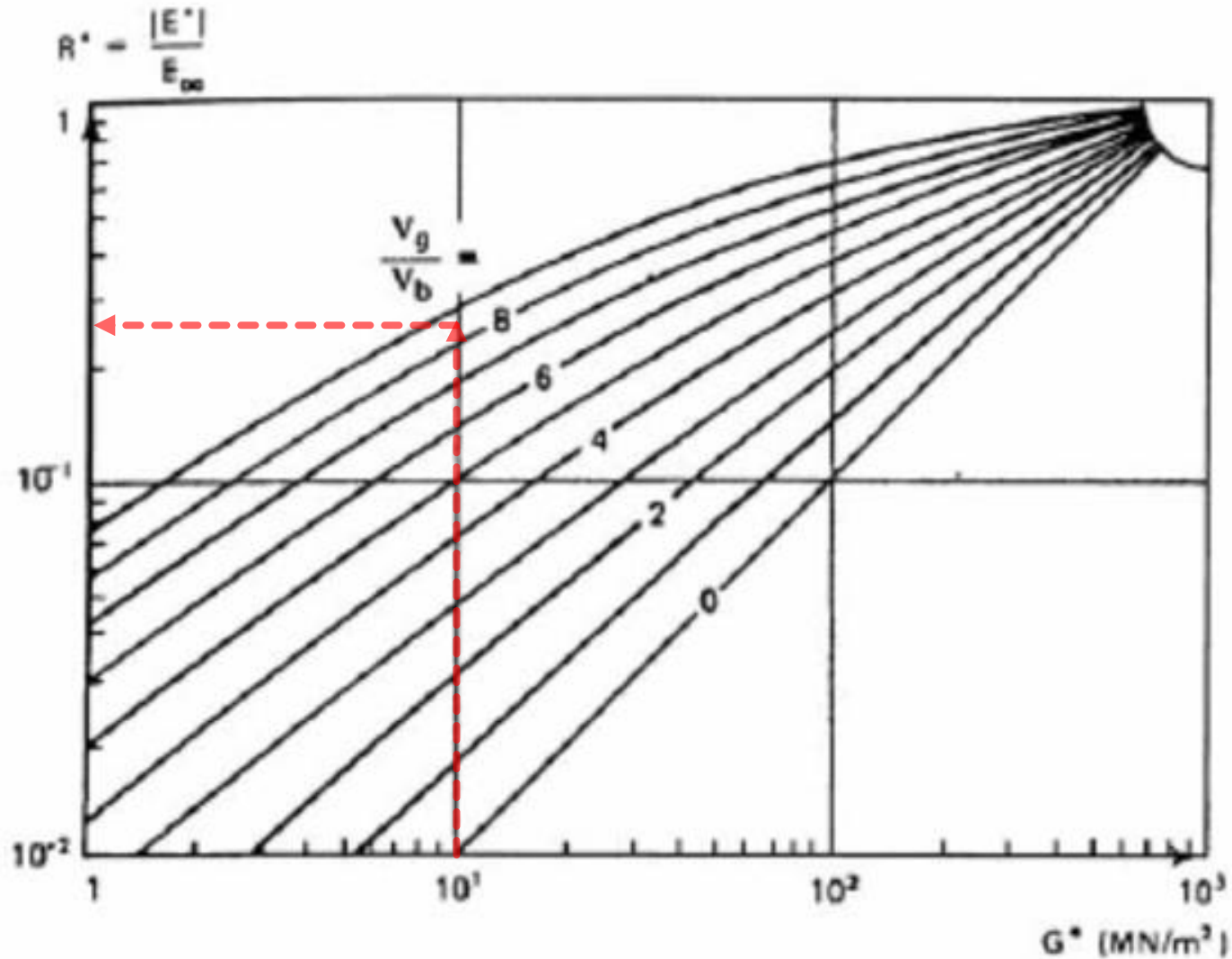


Figure 79: Nomograph of the Belgian Road Research Centre to predict asphalt mixture stiffness.

Example  
Stiffness modulus of the recovered  
bitumen,  $2.2 \times 10^8$  Pa  
Vb: Volume of bitumen, 13.1 %  
Vg: Volume of mineral aggregate, 80.5 %  
Stiffness  
modulus  
of the mix  
 $1.1 \times 10^{10}$  Pa

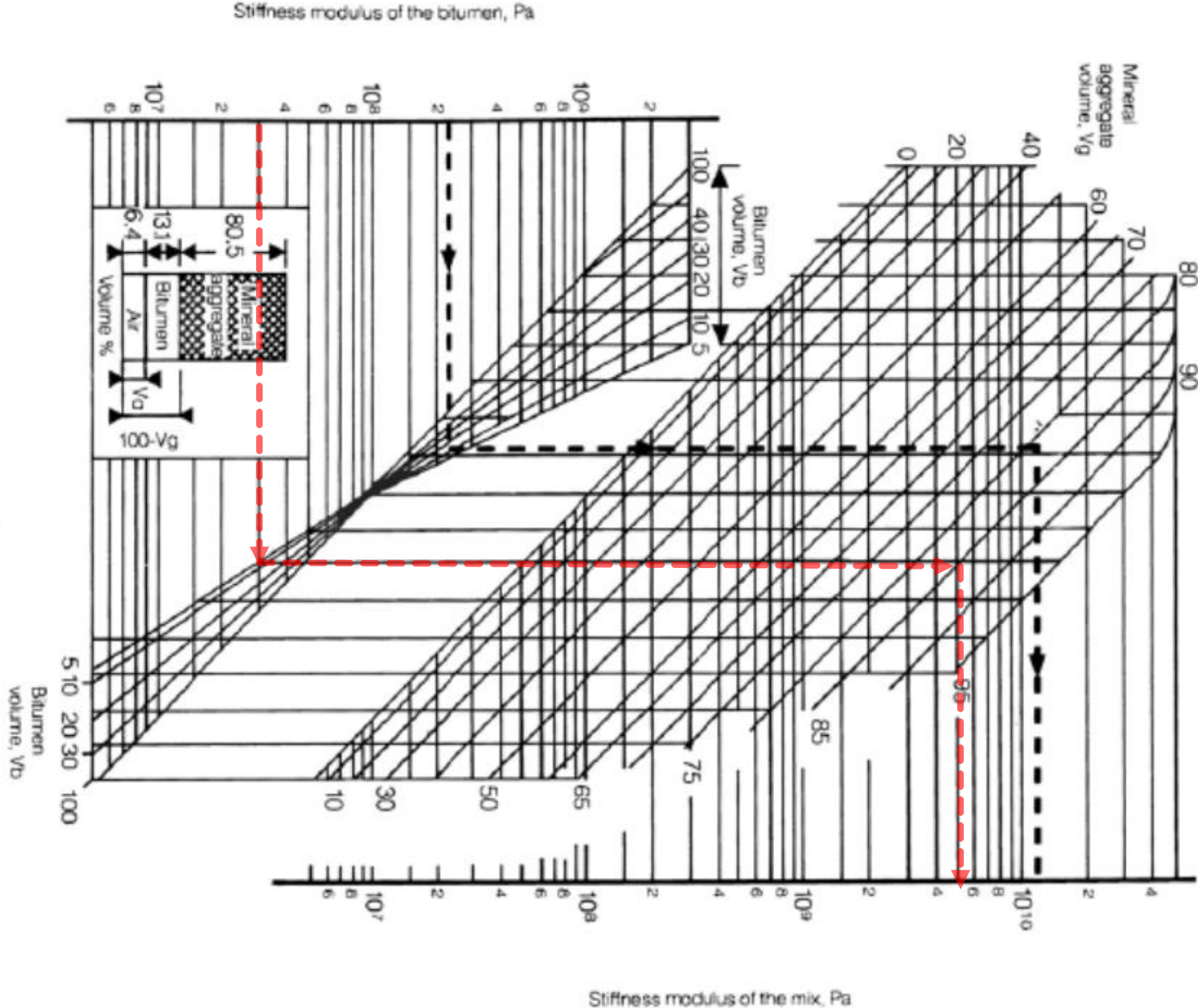


Figure 78: Shell nomograph to predict the stiffness of asphalt mixtures.

- From this comparison it is clear that different values can be obtained using different procedures. The procedure proposed by the Belgian Road Research Centre is preferred since it is based on a larger dataset. It should be noted that in case of elevated pavement temperatures and relatively long loading times, no realistic stiffness values will be predicted using the nomographs. The BANDS program e.g. will give a warning that no value could be determined. The question now is what to do in those situations.
- One recognizes that at elevated temperatures and long loading times, the behaviour of the asphalt mixture strongly depends on the characteristics of the stone skeleton especially in case of stone skeleton mixtures like stone mastic asphalt (SMA) and porous asphalt concrete (PAC). Furthermore one knows that under those conditions, asphalt mixtures are prone to permanent deformation.



Research done by Antes e.a. [33] has shown that the stiffness modulus of asphalt mixtures becomes stress dependent at elevated temperatures. This dependency can be modeled as follows:

$$M_r = k_1 \{(\sigma_3 + k_3) / \sigma_{30}\}^{k_2}$$

Where:

$\sigma_3$  = confining pressure [kPa],

$\sigma_{30}$  = reference pressure = 1 kPa,

$k_1, k_2, k_3$  = constants,

$M_r$  = resilient modulus = 0 if  $\sigma_3 \leq -k_3$ .

Some results are shown in table 15.

Mixture type	Test temperature [ $^{\circ}\text{C}$ ]	Loading frequency [Hz]	$k_1$	$k_2$	$k_3$
STAC	40	25	0.0008	1.879	3143.40
		8	0.0008	1.894	2408.23
		0.5	0.0002	2.054	1600.58
	50	25	0.0002	1.929	2795.66
		8	0.0003	1.945	1880.27
		0.5	0.0001	2.104	1592.74
PAC	40	25	0.0006	1.925	2065.65
		8	0.0008	1.890	1681.70
		0.5	0.0003	2.029	1362.47
	50	25	0.0005	1.971	1347.48
		8	0.0006	1.928	1206.74
		0.5	0.0003	2.050	1052.94
DAC	40	25	0.0005	1.835	4518.63
		8	0.0004	1.926	2579.78
		0.5	0.0001	2.141	1845.23
	50	25	0.0003	1.835	4518.63
		8	0.0002	2.020	1828.18
		0.5	0.0001	2.141	1845.23

Table 15: Constants of the stress dependent resilient modulus for three asphalt mixtures.

Table 16 gives some details on the composition of the mixtures.

Property	STAC	PAC	DAC
Bitumen content [% m / m] "on" 100% aggregate	4.6	4.6	5.9
Pen of recovered bitumen	33	64	31
Void content [%]	5.5	18.1	4.2
Degree of compaction [%]	98.7	104.5	99.4

Table 16: Composition of the mixtures of table 15.

Some results are also shown in tables 17 and 18.

T [°C]	f [Hz]	$\sigma_3 = 0$ kPa	$\sigma_3 = 300$ kPa	$\sigma_3 = 590$ kPa
30	0.1	1034	1374	1882
30	8	4012	4681	5465
30	25	6128	6731	7608
40	0.5	935	1254	1789
40	8	1981	2437	3084
40	25	3027	3582	4198
50	0.5	652	845	1386
50	8	907	1153	1669
50	25	1230	1651	2337

Table 17: Stress dependent stiffness modulus for STAC as determined by means of repeated load triaxial tests.

T [ $^{\circ}$ C]	f [Hz]	$\sigma_3 = 0$ kPa	$\sigma_3 = 300$ kPa	$\sigma_3 = 590$ kPa
30	0.3	635	1069	1502
30	8	1999	2312	2783
30	25	3027	3366	4041
40	0.5	816	1188	1567
40	8	1435	1624	2014
40	25	1931	3131	2641
50	0.5	721	886	1191
50	8	815	986	1318
50	25	908	1106	1431

Table 18: Stress dependent stiffness modulus for PAC as determined by means of repeated load triaxial tests.

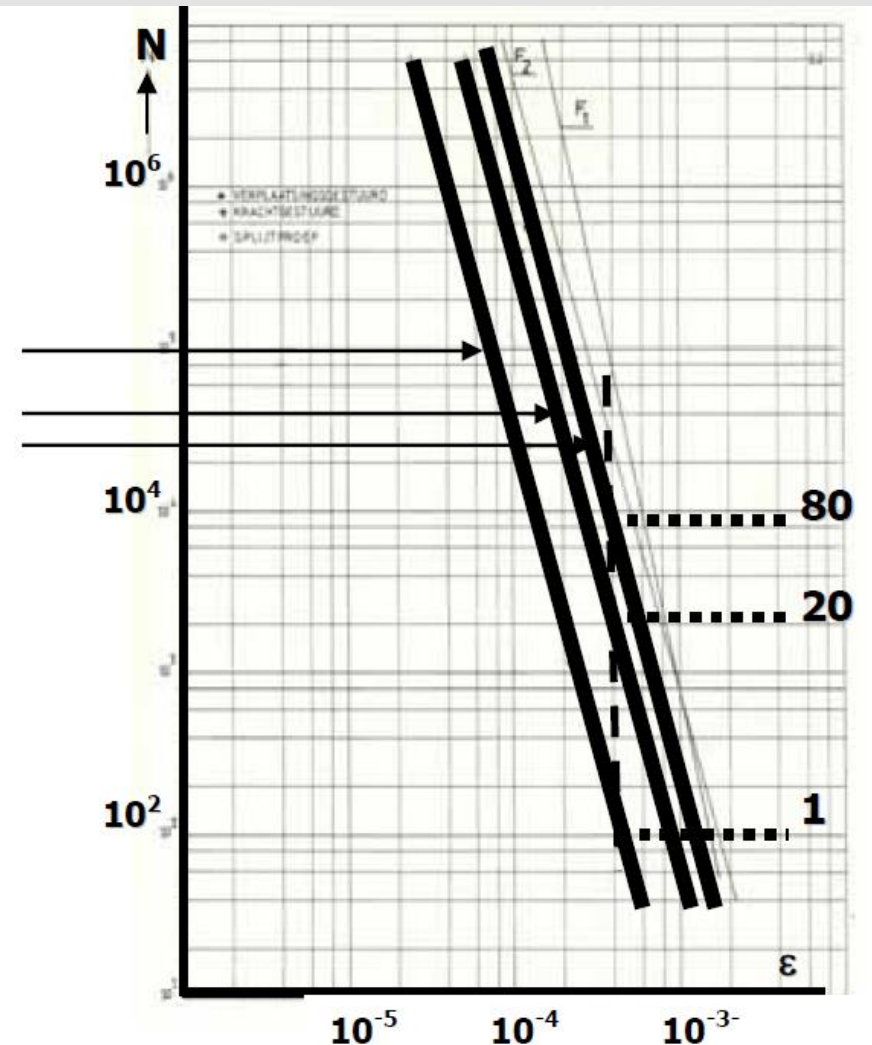
The values shown in tables 17 and 18 can be used to make a first estimate of the stiffness modulus for permanent deformation analyses.

### 8.3 Fatigue resistance

Fatigue tests are also done using the equipment shown in figure 76. The type of fatigue test influences the test result. This is e.g. shown in figure 82 where results of three different types of test as performed on the same mixture are shown.

indirect tension test  
4p bending constant load  
4p bending constant displacement

Figure 82: Fatigue relations obtained by means of different tests





From this figure it becomes quite clear that the intercept value  $k$  of the fatigue relation

$$N = k (1 / \epsilon)^n$$

is rather a specimen property than a material property. As mentioned in the lecture notes on asphalt materials, the slope of the fatigue line  $n$ , is a material property and depends on the slope of the master curve for the complex modulus (the ratio of stress to strain under vibratory conditions) of the mixture. It has been shown [34] that  $n$  can be determined using:

$$n = 2 / \{ m (0.541 + 0.346 / m - 0.0352 V_a) \}$$

Where:

$m$  = slope of the  $\log t$  vs  $\log E^*$  relationship,

$V_a$  = void content [%].

For 4 point bending fatigue relationships as determined by means of constant displacement type of tests, it was determined [34] that the intercept value  $k$  can be estimated using:

$$\log k = 6.589 - 3.762 n + 3209 / E^* + 2.332 \log V_b + 0.149 V_b / V_a + 0.928 \text{ PI} - 0.0721 T_{\text{R\&B}}$$

Where:

$E^*$  = complex modulus [MPa],

$V_b$  = volume percentage of bitumen [%],

PI = penetration index.

TR&B = softening point [ $^{\circ}\text{C}$ ].

- In order to find a k value which is applicable for practical situations, the k value as obtained in the lab or by means of the above mentioned equation should be multiplied with a constant that takes into account the effect of
  - ❖ healing of the asphalt mixture,
  - ❖ lateral wander of the traffic loads and
  - ❖ geometrical differences between the beam and the actual pavement.

Healing of the asphalt mixture has to do with the fact that asphalt mixtures have the capacity to “repair” themselves. This self repairing mechanism occurs when the material is not subjected to loading and it has been shown that especially the ratio duration of the rest period : duration of the loading period is of importance. If this ratio is about 20, the self repairing capacity has reached its maximum.

Furthermore healing depends of course on the amount and type of bitumen used in the mixture. It can be shown that especially the maltene phase of the bitumen is responsible for healing implying that softer bitumens show a better healing performance than harder bitumens. Figure 83, developed from data presented by Francken [35], shows the effect of the amount of bitumen on healing, while figure 84 [36] shows the effect of the type of bitumen.

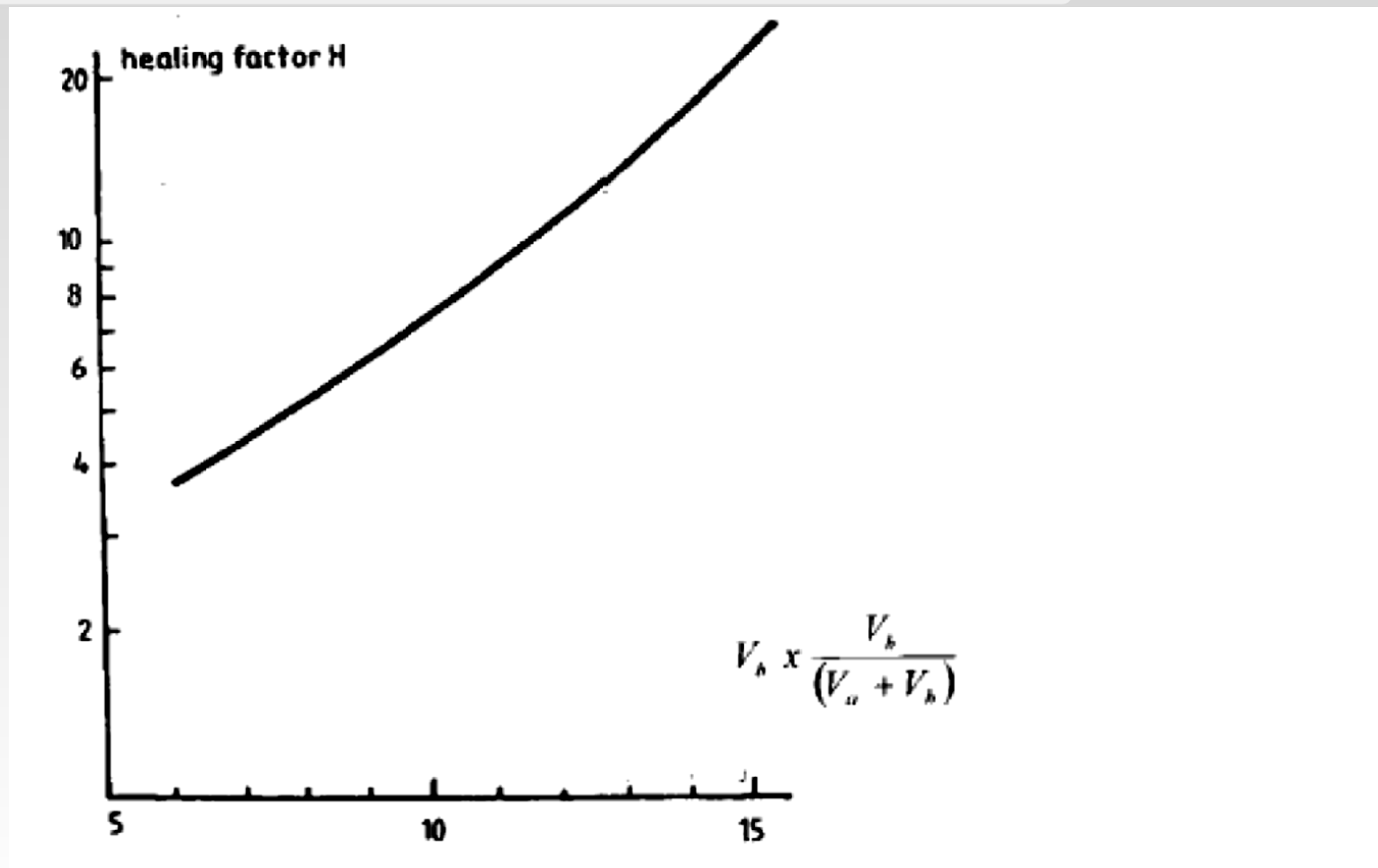


Figure 83: Effect of the amount of bitumen expressed as  $V_b \times V_b / (V_a + V_b)$  on healing.

Note:  $V_b$  and  $V_a$  are given as percentages.

The term  $V_b / (V_b + V_a)$  as used in figure 83 is known as the degree of filling of the voids in the aggregate skeleton with bitumen. Figure 83 is develop from data obtained on four mixtures having bitumens with a penetration ranging between 47 and 80.

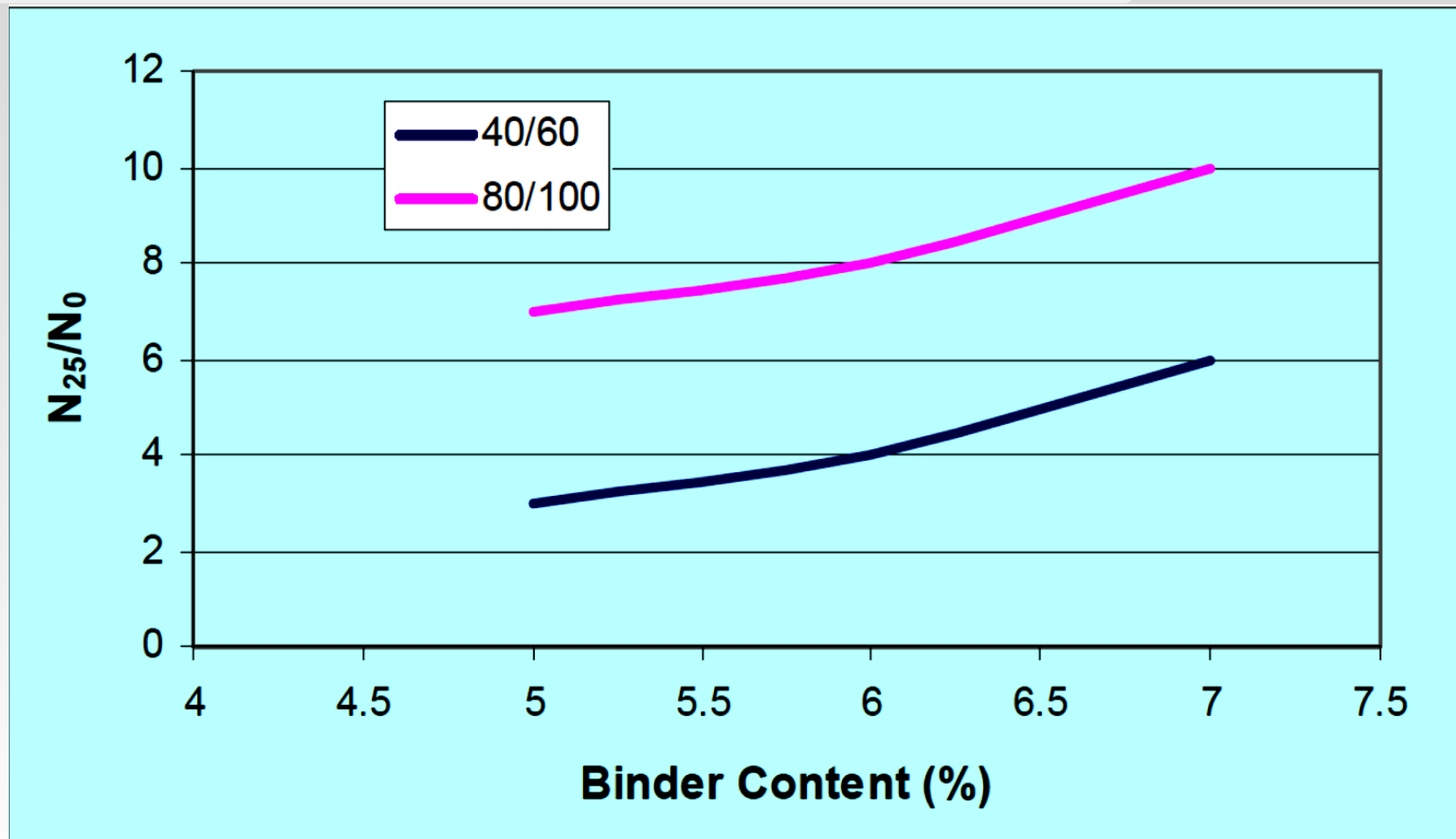
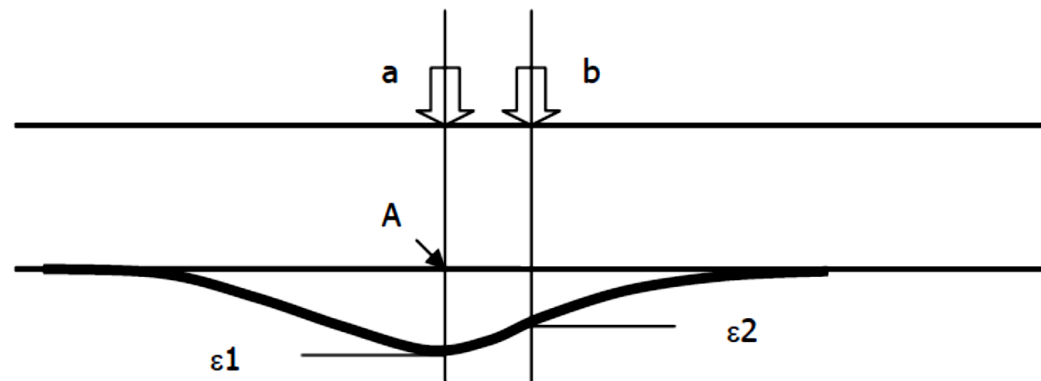


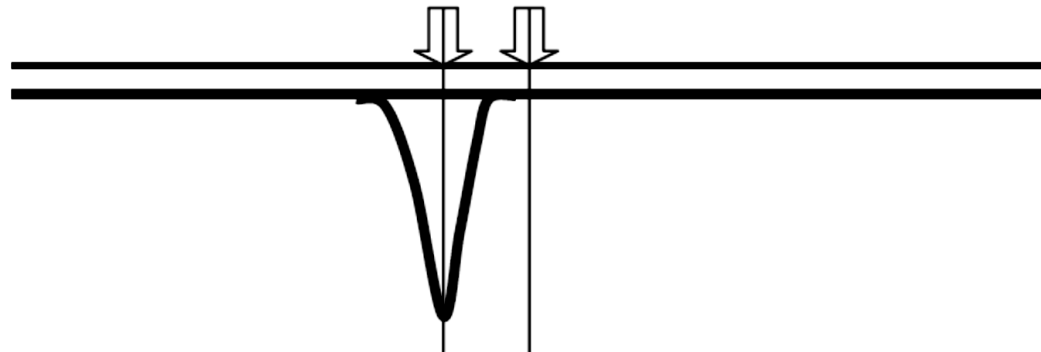
Figure 84: Influence of bitumen content and type of bitumen on healing of asphalt mixtures.

Note:  $N_{25}$  means the nr. of load repetitions to failure with a rest period/loading period ratio of 25.  $N_0$  means nr. of load repetitions to failure when no rest periods are applied.

- It is a well known fact that cars and trucks don't drive in a perfectly straight line; in practice some **lateral wander** always occurs.
- Because of this lateral wander, the maximum stresses and strains don't always occur in the **same location**.
- This again implies that the allowable number of wheel passages is actually larger than the number of peak tensile strain repetitions that can be taken in a specific location.



The load at position a causes a tensile strain  $\epsilon_1$  in location A, the load in position b still causes a tensile strain  $\epsilon_2$  in point A. The effect of lateral wander is therefore limited.

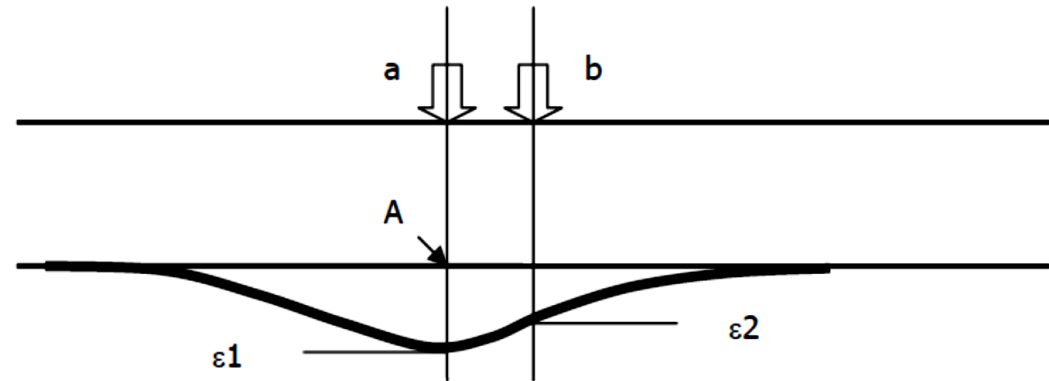


In this case the load in position b causes no tensile strain in location A. The effect of lateral wander is therefore large.

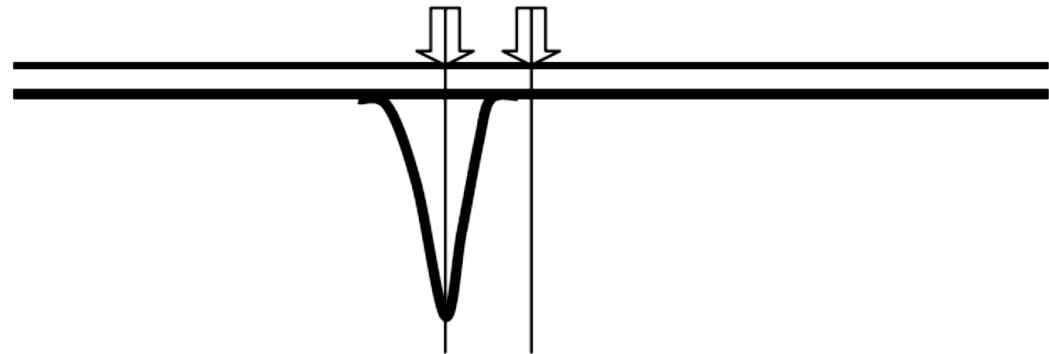
Figure 85: Principle of the effect of lateral wander.



- The amount of lateral wander that occurs depends mainly on the lane width.
- Furthermore the stiffness of the pavement determines the load spreading and determines whether e.g. the tensile strain is fairly constant at the bottom of the asphalt layer or whether high strains occur locally (see figure 85).



The load at position a causes a tensile strain  $\varepsilon_1$  in location A, the load in position b still causes a tensile strain  $\varepsilon_2$  in point A. The effect of lateral wander is therefore limited.



In this case the load in position b causes no tensile strain in location A. The effect of lateral wander is therefore large.

Figure 85: Principle of the effect of lateral wander.

CROW [37] has developed a procedure to estimate the positive effect of lateral wander. This procedure is outlined hereafter. First of all, the radius of relative stiffness is calculated using:

$$L_k = [E_1 h_1^3 (1 - v_s^2) / 6E_s (1 - v_1^2)]^{0.33}$$

Where:

$L_k$  = radius of relative stiffness [mm],  
 $E_1$  = stiffness modulus of the asphalt layer [MPa],  
 $E_s$  = stiffness modulus of the subgrade [MPa],  
 $v_1$  = Poisson's ratio of the asphalt layer,  
 $v_s$  = Poisson's ratio of the subgrade.

Figure 86 is then used to determine the lateral wander that will occur. That number together with  $L_k$  is then used in figure 87 to determine the correction factor on pavement life due to lateral wander.

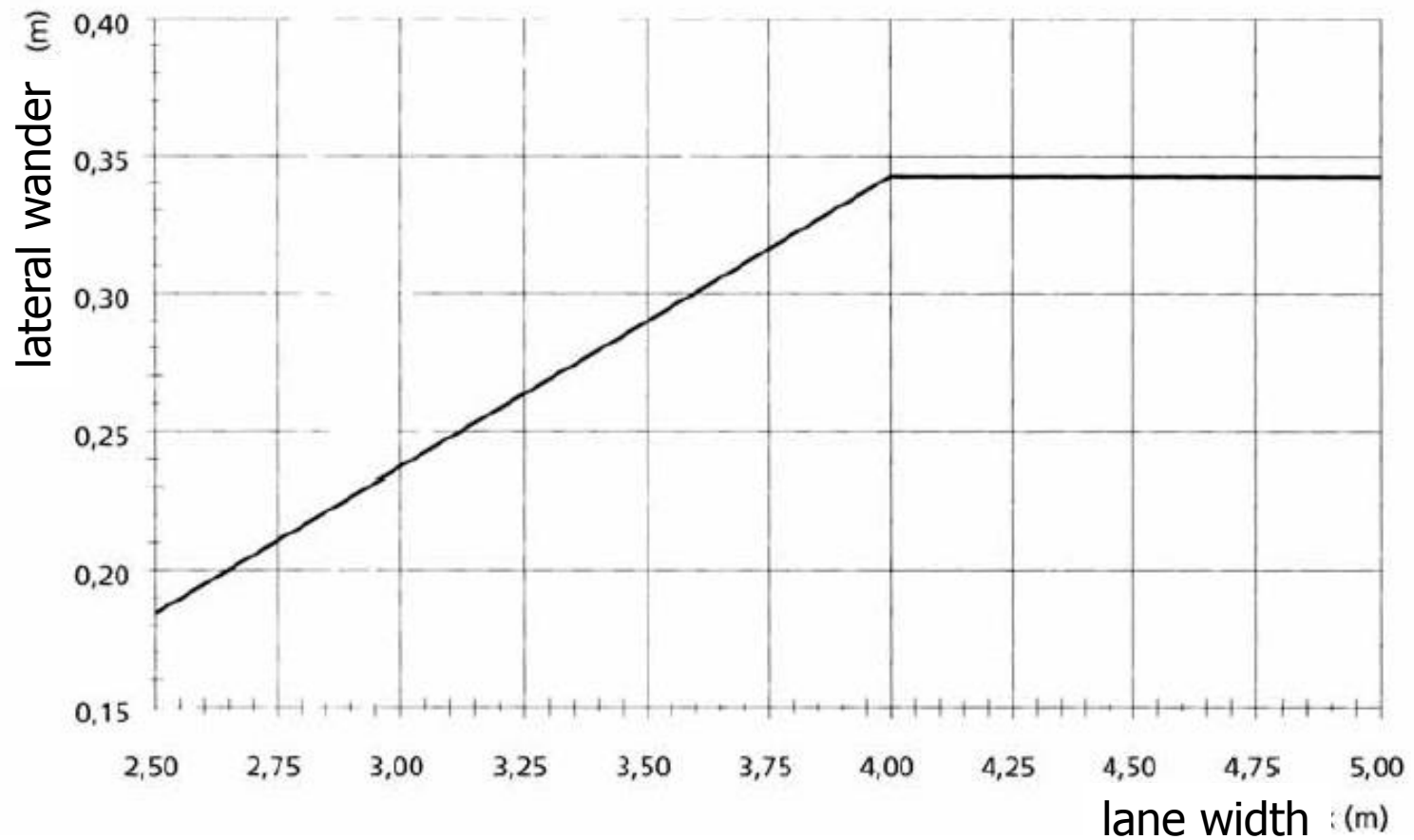


Figure 86: Lateral wander in relation to lane width.

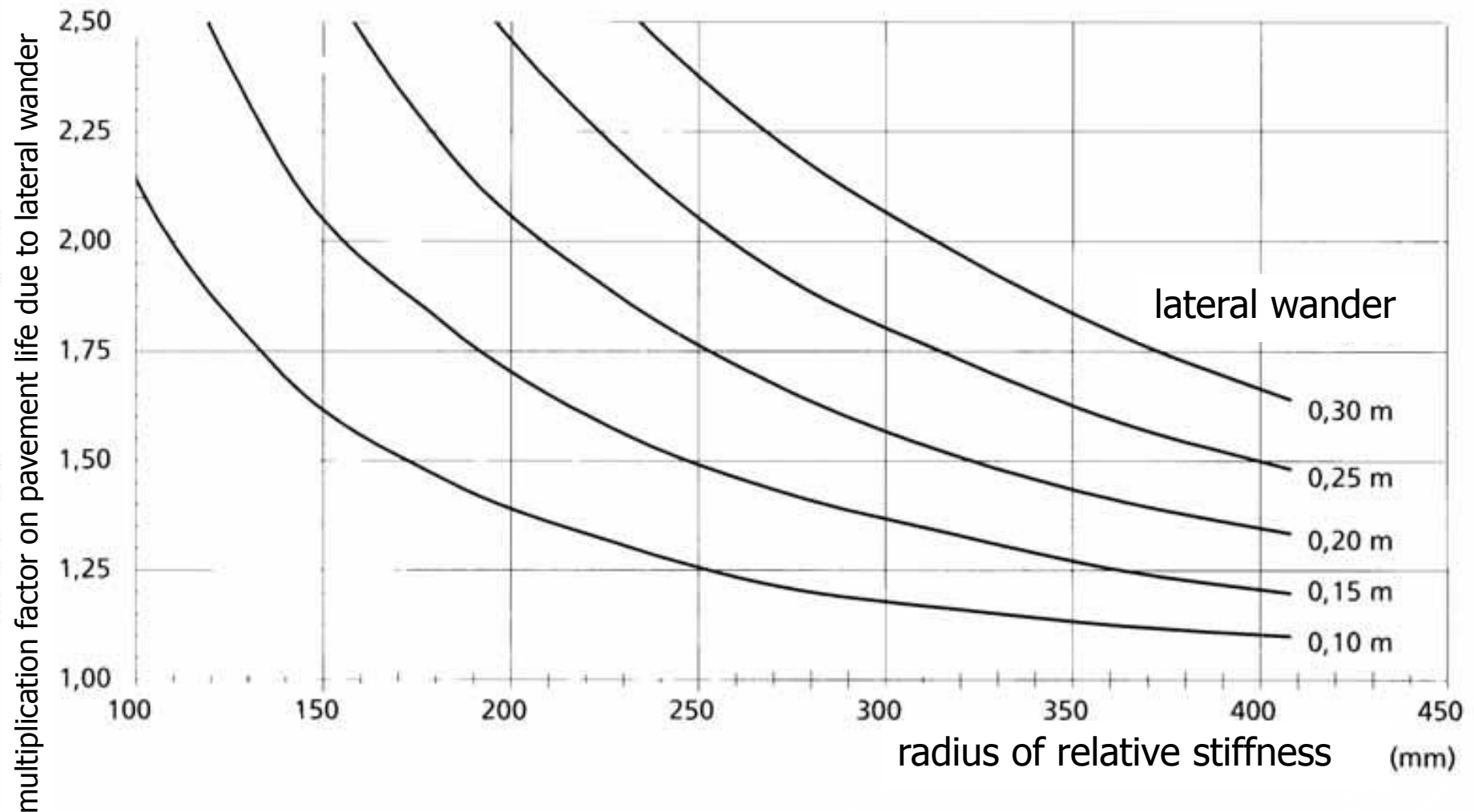


Figure 87: Correction factor on pavement life as a function of the lateral wander and pavement stiffness.

Having discussed the correction factors that should be applied on the laboratory fatigue relation as a result of lateral wander and healing, attention should now be paid to the correction factor that is needed because of geometrical effects. Work done by Groenendijk [22] indicates that the commonly used fatigue relation:

$$N = k \epsilon^{-n}$$

can be rewritten in:

$$N = \alpha h \epsilon^{-n} / (A S_{\text{mix}}^n)$$

Where:

$N$  = number of load repetitions to failure,

$S_{\text{mix}}$  = mixture stiffness,

$h$  = height of the beam,

$A$  = material constant,

$\alpha$  = function which value depends on extent of damage growth in the beam.



- This relationship indicates that the life of a 100 mm thick beam is twice of that of a 50 mm thick beam. This however doesn't necessarily mean that the number of load repetitions to failure of a 100 mm thick asphalt pavement is twice the lifetime of a 50 mm thick beam when subjected to the same strain level.
- In order to be able to relate laboratory fatigue to pavement fatigue, one should have detailed information on both lab fatigue and field fatigue and such data is not readily available. Analysis of the LINTRACK accelerated pavement test data as presented by Groenendijk however showed that the effect of a different geometry between the laboratory fatigue beam (thickness 50 mm) and the test pavements could be written as:

$$GF = 1.33 * 10^{-4} h^2 + 0.0133 h$$

Where:

GF = geometry factor,

h = thickness of the asphalt layer [mm].

In the analysis, the effect of lateral wander could be accurately determined while the healing factor was estimated to be 4 which is a realistic value for the base course mixture that was used in the LINTRACK experiments. It should be noted however that 20% of the pavement surface showed cracking at the end of the pavement life. Given the fact that the GF factor calculated in this way is rather large and is related to extensive cracking, it is suggested to define a practical geometry factor (PGF) as:

$$\text{PGF} = (h - 50) / 50$$

Where:

$h$  = asphalt layer thickness [mm].

In conclusion one can state that the fatigue life of the asphalt layer in a pavement can be calculated using:

$$N = LW * H * \text{PGF} * N_{\text{lab}}$$

Where:

$N$  = in situ fatigue life,

$LW$  = correction factor due to lateral wander,

$H$  = correction factor due to healing,

$\text{PGF}$  = practical geometry factor.

## 8.4 Resistance to permanent deformation

- The resistance to permanent deformation of asphalt mixtures is an important issue since it affects driving comfort and traffic safety. Since the permanent deformations are a results of viscous and plastic deformation, models that allow the visco-plastic behavior to be taken into account should be used to determine the amount of permanent deformation that develops in the pavement. It is therefore quite clear that a linear elastic analysis is in fact useless for the prediction of permanent deformation.
- Also linear visco-elastic models are not capable in predicting with a reasonable degree of accuracy for the amount of rutting that will occur in the asphalt layers. In [33] it has been shown that the viscous parameters are highly stress dependent and in [38] it is shown that adopting such an approach grossly underpredicts observed deformations.

- A method analogue to what is common practice in soil mechanics and that also will be used later on in these notes to limit the permanent deformation in aggregate skeletons, is the one by which the permanent deformation is limited by allowing stress levels which are only a certain percentage of the stress level at failure. In short such methods limitations are set to the ratio  $R$  defined as:

$$R = \sigma_1 / \sigma_{1f}$$

Where:

$R$  = allowable stress ratio,

$\sigma_1$  = applied vertical stress at a certain level of confinement,

$\sigma_{1f}$  = vertical stress at failure at the same level of confinement.

Examples of failure envelopes needed for such an approach are given in figure 88, 89 and 90.

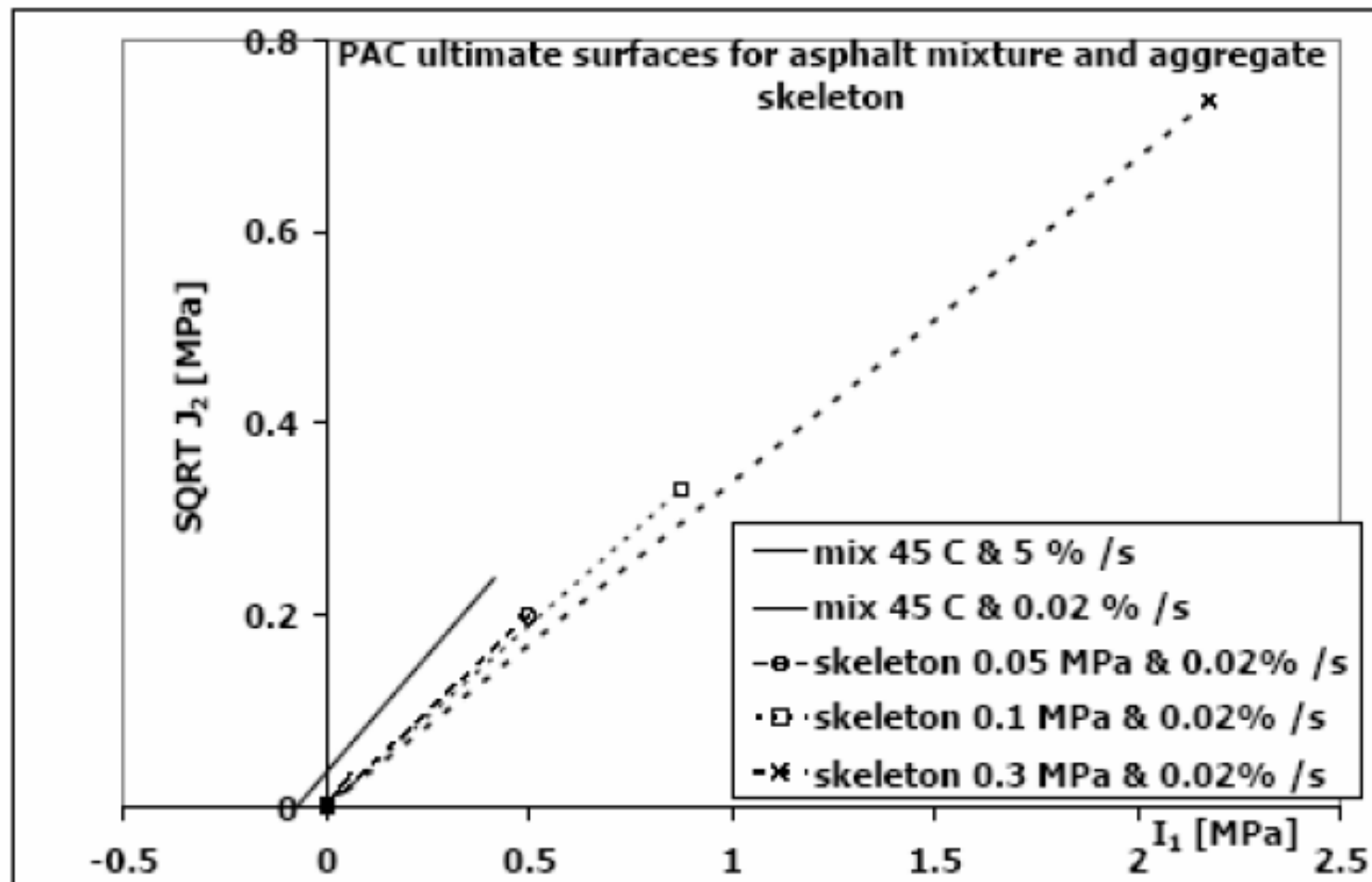


Figure 88: Failure envelopes for a PAC mixture and its skeleton at 45 °C and two strain rates [38].

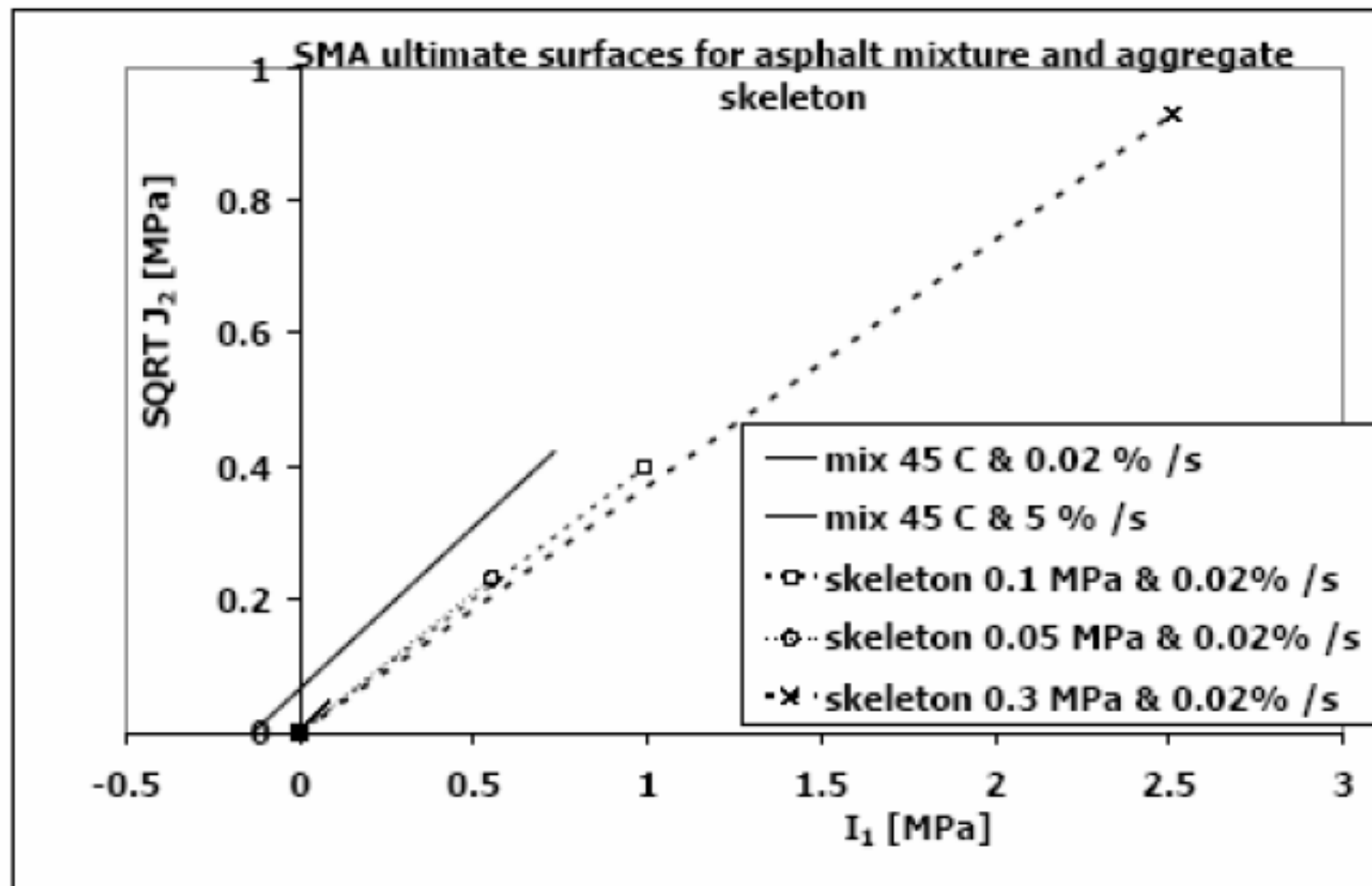


Figure 89: Failure envelopes for a SMA mixture and its skeleton at 45 °C and two strain rates [38].



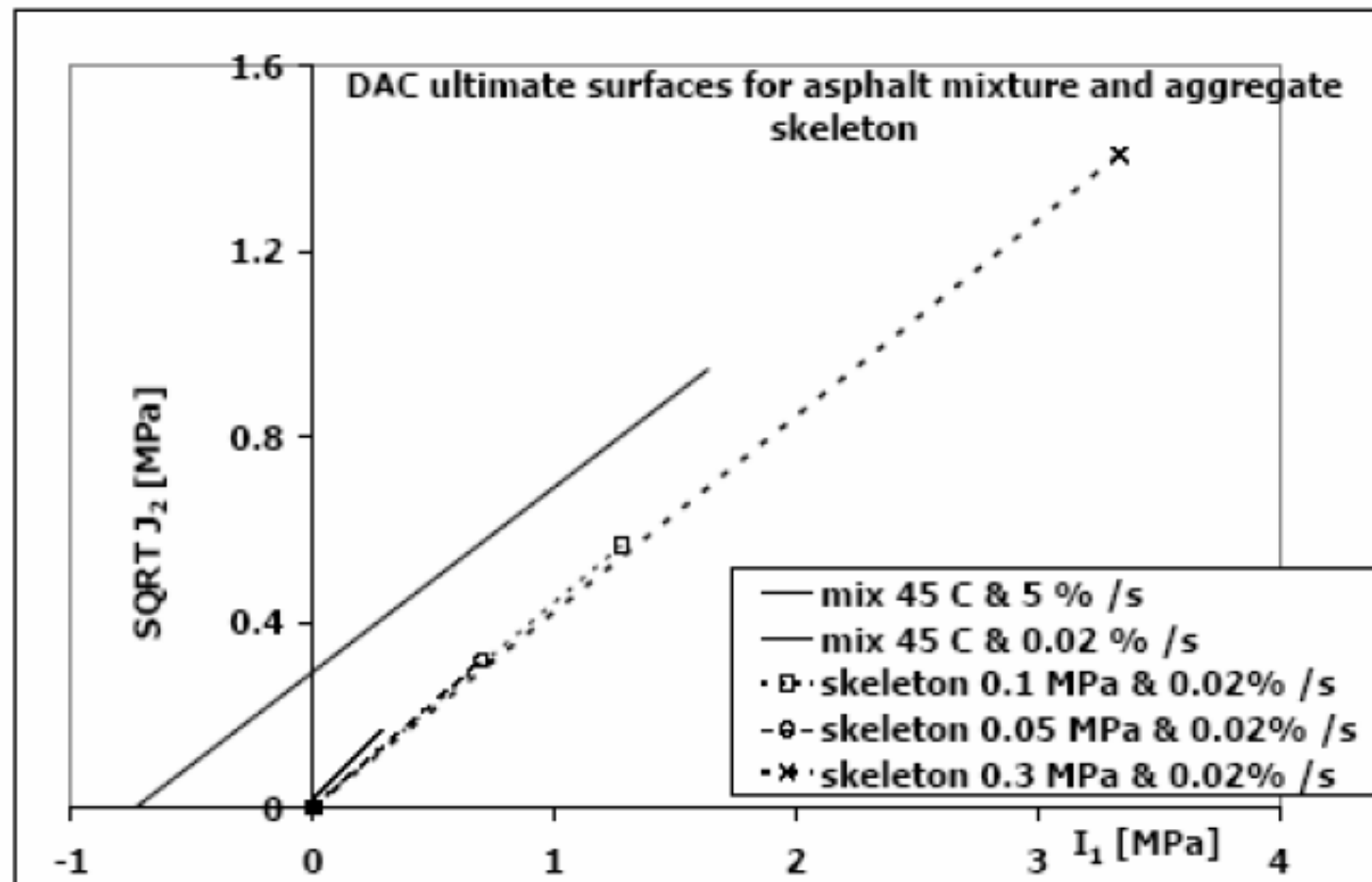


Figure 90: Failure envelopes for a DAC mixture and its stone skeleton at 45 °C and two strain rates [38].

- In [38] it is shown that in SMA and PAC mixtures, stress combinations rather close to the failure envelope can be allowed before significant permanent deformations develop. The allowable stress combinations in the DAC mixture are much lower than those in the SMA and PAC mixture.
- Although this approach certainly has a large potential, it is not yet developed to such a level that it can be used easily for day to day design analyses. Because of that also another approach is presented here which is more or less a hybrid approach since it combines the results of a stress analysis made by means of a multi-layer linear elastic approach and the development of permanent deformation as a function of the applied stresses as observed in the laboratory by means of repeated load testing. This approach is described in great detail in [35].

Francken e.a. [35] have shown that the permanent deformation of asphalt mixtures as determined by means of repeated load triaxial tests can be described by:

$$\epsilon_p = ((\sigma_0 - \sigma_h) / (0.65 E F)) * (t / 1000)^{0.25}$$

Where:

$\epsilon_p$  = cumulative permanent strain,

$\sigma_0 = \sigma_v / 2$ ,

$\sigma_v$  = vertical stress,

$\sigma_h$  = horizontal stress,

$E$  = complex modulus at the given temperature and loading time conditions,

$F = 5.5 * 10^{-2} (1 - 1.02 V_b / (V_b + V_a))$ ,

$V_b$  = volume percentage of bitumen,

$V_a$  = void content,

$t$  = total loading time [s] =  $N f$ ,

$N$  = number of load repetitions,

$f$  = load frequency.

For the time being, this equations is recommended for practical applications.